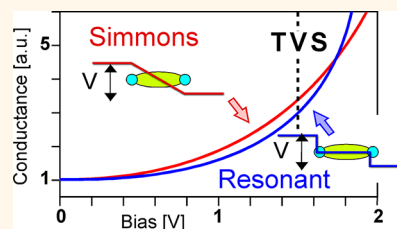# Rethinking Transition Voltage Spectroscopy within a Generic Taylor Expansion View

Ayelet Vilan, * **David Cahen, and Eli Kraisler**

Department of Materials and Interfaces, Weizmann Institute of Science, Rehovot, Israel

ABSTRACT   Transition voltage spectroscopy (TVS) has become an accepted quantification tool for molecular transport characteristics, due to its simplicity and reproducibility. Alternatively, the Taylor expansion view, TyEx, of transport by tunneling suggests that conductance—voltage curves have approximately a generic parabolic shape, regardless of whether the tunneling model is derived from an average medium view (*e.g.*, WKB) or from a scattering view (*e.g.*, Landauer). Comparing TVS and TyEx approaches reveals that TVS is closely related to a bias-scaling factor, V_0, which is directly derived from the third coefficient of TyEx, namely, the second derivative of the conductance with respect to bias at 0 V. This interpretation of TVS leads to simple expressions that can be compared easily across primarily different tunneling models. Because the basic curve shape is mostly generic, the quality of model fitting is not informative on the actual tunneling model. However internal correlation between the conductance near 0 V and V_0 (TVS) provides genuine indication on fundamental tunneling features. Furthermore, we show that the prevailing concept that V_0 is proportional to the barrier height holds only in the case of resonant tunneling, while for off-resonant or deep tunneling, V_0 is proportional to the ratio of barrier height to barrier width. Finally, considering TVS as a measure of conductance nonlinearity, rather than as an indicator for energy level spectroscopy, explains the very low TVS values observed with a semiconducting (instead of metal) electrode, where transport is highly nonlinear due to the relatively small, bias-dependent density of states of the semiconducting electrode.

Quantification of electronic transport across molecules is often hampered by rather featureless current—voltage traces, which can be fitted to a variety of tunneling models. Uncertainties in the exact nanoscale geometry add considerable difficulty to comparing experimental data to results. In practice, most of the reported current—voltage (J—V) data can be fitted over a considerable bias range to a generic parabola.[1,2] This flexibility in fitting of a given J—V trace to vastly different tunneling models severely undermines the credibility of quantification of such electronic transport data. The method of "transition voltage spectroscopy" (TVS)[3] has emerged as an attractive approach, due to its clear merits of reproducibility[4,5] even when the conductance varies by 2 orders of magnitude,[6] and because of experimentally demonstrated correlations between TVS values and molecular energy levels[4] or applied gate bias.[7]

Originally, TVS was derived from the Fowler—Nordheim description of charge transport by field-emission tunneling,[3] where the function FN should be linear with $1/V$:

$$FN = \ln(J/V^2) \qquad (1)$$

Beebe *et al.* were the first to observe that a minimum in an FN($1/V$) plot is highly reproducible for molecular junctions and, thus, may serve as a a molecular fingerprint.[3] They termed this min(FN) as "TVS" and assumed that because FN itself is monotonic (linear with $1/V$), a minimum in FN must imply a transition from deep-tunneling into field-emission transport. Such a transition is expected (see SI eq S12) when the applied bias equals the energy difference between the electrode's Fermi level and the nearest molecular energy level, or the barrier height (ε).[8] The idea that an experimentally accessible and reproducible TVS is directly related to the barrier height for charge transport made it extremely appealing. An observed correlation between TVS and energy levels of a set of conjugated molecules supported the use of TVS as a genuine characteristic of molecular transport.[4]

©2012 American Chemical Society

a) Conducting Bridge
Step-like Potential

Off / Tail Resonance   Resonance

b) Insulating Bridge
Trapezoidal Potential
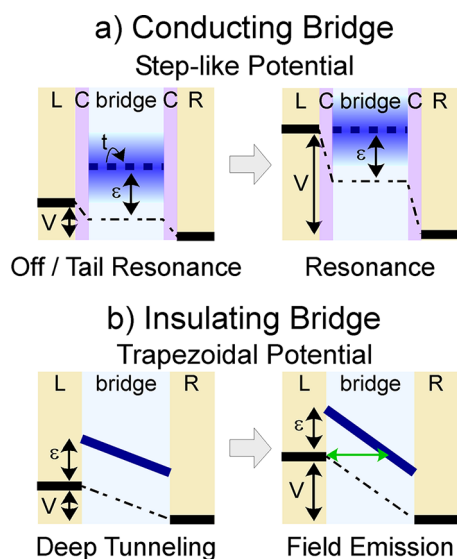

Deep Tunneling   Field Emission

Figure 1. Schemes of different tunneling models for two extreme cases of potential profiles: (a) *step-like* **profile for a case where the bridge is much more conducting than the contacts and (b)** *trapezoidal* **for a case where the bridge is the main resistance of the junction. The two left panels are the low-bias case, and the two right panels describe a high-bias case. L and R are the left and right electrodes, with Fermi energy marked by a thick black line, and C stands for contact. Dotted line illustrates the potential profile, while the thick blue line marks the molecular level, which could be either broadened (varying tone in a) or a sequence of localized states (broken line in a). Field emission (b, right side) is characterized by a tunneling distance (green arrow) that is shorter than the full electrodes' separation.**

These merits of TVS made it an important bridge between experiments and theory, but the concept of field emission cannot be reconciled with the notion of a molecular wire. An important issue is the potential profile. A transition in transport mechanism into field emission implies that the bias falls on the insulating medium ("bridge") to form a trapezoidal potential profile (Figure 1b). In contrast, most molecular models assume the *contacts* to be the least conducting link, with a potential jump across them and a flat potential along the rather conductive bridge (Figure 1a; see, however, refs 9, 10 for theoretical works that consider a trapezoidal potential). This has led to a large theoretical effort to predict a minimum in the FN presentation of current−voltage characteristics within the Landauer formalism.[9−14] These studies have generally shown that not only is TVS related to the barrier height but it is also sensitive to other factors such as the asymmetry of the junction,[10,13,15] coupling to the electrodes,[10] molecular length (tunneling distance or width of the barrier),[10] and potential profile across the junctions.[10] Thus, it has become accepted that TVS marks the bias at which the tail of the peak of the molecular transmission function comes into resonance with the electrode's Fermi level.[9]

We promote a different view, namely, that of TVS as a scaling factor for the applied bias or as a measure of the strength of the nonlinearity of the conductance with respect to bias. Namely, TVS is an intrinsic characteristic of transport by tunneling at any bias, regardless of any onset or transition in transport mechanism. Viewing TVS as a bias scaling factor not only substantiates the use of TVS as a genuine tunneling characteristic rather than a mathematical artifact[14] but also stresses that TVS expresses the combined effect of several possible junction characteristics and does not necessarily reflect spectroscopic details.

Our interpretation of TVS is based on performing a Taylor expansion, TyEx, of the conductance $G(V)$ around $V = 0$. This procedure can be applied to basically any tunneling model. A three-term TyEx of conductance−voltage ($G−V$) relation was the prevailing approach in the 1960s and 1970s for WKB-based tunneling models,[16,17] and observing a parabolic $G−V$ curve was even included in the list of criteria for identifying tunneling.[18,19] We show that TVS is directly related to the third TyEx coefficient or the second derivative of conductance with respect to bias at 0 V. This TyEx coefficient is best considered as a bias-scaling factor, V_0 (in V). Earlier we defined a parameter called "shape factor" (ρ, in 1/V),[1,2] which is approximately the reciprocal of V_0. Here we prefer to use V_0 over ρ in analogy with TVS.

Since such expansion is only an approximation, TVS should be generally viewed as a bias-dependent perturbation of V_0, leading to TVS values that are up to 50% smaller than V_0. This report focuses primarily on the conceptual view of TVS and does not aim at replacing detailed TVS interpretations.[9,10,12,13,20]

An important advantage of V_0 over TVS is its simple mathematical expression that allows evaluating the relevance of different tunneling models to experimental data. In this report we provide a few analytical expressions for V_0 ($\approx$TVS), based on TyEx of different accepted tunneling models, assuming either trapezoidal (Figure 1b) or step-like potential (Figure 1a) profiles, with either resonant or off-resonant tunneling, or based on a solid-state view (effective mass) or molecular view (coupling). The results show that the assumed correlation between TVS and barrier height is correct only for the specific case of resonant tunneling.[10] For off-resonant, TVS is generally proportional to the ratio between the barrier height and barrier width, as we observe experimentally for junctions made of alkyl-phosphonate monolayer on oxidized Al contacted by Hg. Finally, we consider TVS for nonmetallic electrodes, such as Si. We show that even in cases of heavily doped Si and symmetric $J−V$ curves, the Si electrode dictates much of the shape of the $G−V$ curves due to its limited density of states at the Fermi level. Therefore, for nonmetallic electrodes, TVS is a complicated function of both molecular and electrode parameters and is not very informative.

The following section considers the mathematics behind TVS. On the basis of simulated $J−V$ curves we show that no transition in transport occurs at TVS.

We then compare between TVS and TyEx results and show that $TVS^{-2} \approx (d^2G/dV^2)|_{V=0}$ and derive TyEx coefficients for different tunneling models and specifically consider the issue of length-dependent TVS. The next section illustrates how the correlation between bias scaling (V_0 or TVS) and conductance scaling can be used to extract tunneling information from experimental data, and finally we show the inapplicability of TVS to systems with nonmetallic electrodes, such as heavily doped Si.

TVS Is Not Transition-Related. The clear minimum in TVS plots (FN *vs* $1/V$) gives the impression of a drastic change, originating in, for example, entrance into a resonant window of allowed energy levels.[9] The first message we wish to convey is that, in general, both the current density, J, and its first derivative with respect to bias, the conductance, G, are smooth and continuous as the applied bias is scanned across the TVS value.[9] The observed minimum has a different origin than an actual change in transport mechanism. To demonstrate this, we simulated four $J-V$ curves using vastly different tunneling models, but with the parameters for each model chosen in such a way that all curves have an identical TVS value of 1.5 V. We note that the choice of tunneling parameters that gives a specific TVS value is not obvious and is based on the TyEx as described later. Variations in net conductance were ignored, and therefore all curves have $G(0) = 1$. While there are significant differences between the models below, all are versions of coherent tunneling. The models were as follows:

(I) Simmons model[8] with a genuine transition into field emission at TVS. The Simmons model describes what is called deep tunneling. The model originates from a solid-state view of transport, *i.e.*, delocalized energy levels and free-charge carriers with an effective mass. According to this model, a transition into field emission would occur when the applied bias equals the energy barrier height.

(II) Simmons model[8] with a false minimum, *i.e.*, the minimum of the FN function (eq 1) occurs at a bias voltage that is lower than the voltage (*i.e.*, the barrier height) at which the actual transition into field emission occurs.

(III) Off-resonant sequential tunneling. In this model, derived by Mujica and Ratner,[21] there is no direct coupling between the two electrodes, but rather a sequential coupling along the bridge sites. This model should not be confused with hopping, because the transport is coherent and the electron does not occupy the bridge states as in hopping.[21]

(IV) Tail-broadening resonant tunneling as derived by Huisman *et al*.[11] where the two electrodes are directly coupled. The coupling strength and, thus, the level broadening decay exponentially with the tunneling distance.

In the Supporting Information we provide the mathematical equations for each model. Complications such as asymmetry are deliberately ignored here. The justification to consider the WKB-based Simmons model[8] is first because the TVS concept originally emerged from this model, which is still widely used. Second, the Simmons model represents the case where the potential drops on the bridge rather than on the contacts, also known as trapezoidal potential profile (Figure 1b). DFT computations indicate that the potential profile has a drastic effect on TVS values.[9,10] However, the "trapezoidal" profile, where most of the bias falls on the bridge, is rarely considered in recent analytical models, which mostly assume the "step" profile, where the potential changes mainly at the contacts. At the other extreme is the tail-resonant model, derived by Huisman *et al.*,[11] which represents a variety of recent Landauer-based models.[9,12,13,20] We preferred this model because of its relative simplicity. Finally, off-resonant, sequential tunneling, derived by Mujica and Ratner,[21] represents an intermediate case, where the bridge is equipotential (step potential profile) as in the resonant-tunneling model, but assumes a sequence of localized bridge states without direct coupling between left and right electrodes, *i.e.*, with a pronounced bridge effect, similar to WKB models.

Figure 2a shows that only for a genuine transition into Fowler−Nordheim transport (curve I, black) is there an observed change in current at V = TVS (1.5 V, vertical dotted line), which is further observed as a sharp jump in the $G-V$ curve presentation (Figure 2c). A genuine transition to field emission (curve II, red) or onset of resonance with maximal transmittance (curve IV, light blue) could be also observed but at a much larger voltage than TVS. Nevertheless, all data show a clear minimum in a Fowler−Nordheim presentation (Figure 2b, eq 1), where the genuine Fowler−Nordheim curve (curve I, black) differs only in its strong asymmetry and linear behavior for V > TVS. Moreover, fixing TVS at a given value (1.5 V) made the four curves almost overlap each other over a large bias range (after scaling the current magnitudes; curves in all panels of Figure 2 are vertically shifted; otherwise they would be almost indistinguishable). We conclude that TVS does not mark a change in transport mechanism; on the contrary, TVS is a genuine expression of transport by tunneling over a wide bias range. Therefore, a TVS minimum is not a mathematical artifact,[14] because it contains key information on the shape of the $G-V$ (or $J-V$) curves. Thus, similar to the commonly used decay length, β, TVS should be used as an empirical parameter that can be highly characteristic for a given junction, even though it can be interpreted in various ways, as will be discussed next.

TVS Reflects the Nonlinearity of the Transport. If TVS occurs in a perfectly smooth region of the $G-V$ curve, it must originate in a mathematical minimum of the FN curve, which is directly derived from differentiating the Fowler−Nordheim presentation, FN (eq 1), with
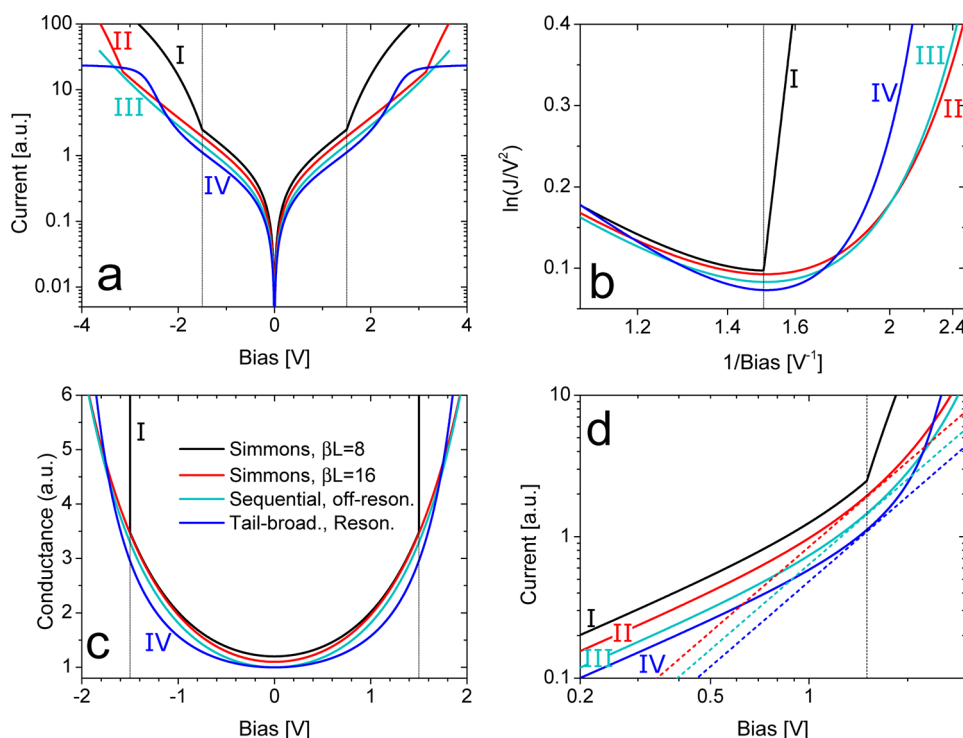
Figure 2. Different presentations of simulated current−voltage curves, showing (a) the simulated current over a wide bias range; (b) "Fowler−Nordheim" presentation of the same curves (eq 1); (c) conductance plots, i.e., the first derivative of (a); and (d) log−log plots of (a) at high bias. Tangential, dotted lines in (d) show $J = AV^2$ lines for arbitrary A values. In all panels current values were arbitrarily scaled and shifted for clarity. The transport parameters were chosen to give TVS = 1.5 V, marked by a vertical dotted line in all panels. Each of the four curves in each panel represents a different model as detailed in the text: (I) Simmons with a real transition into field emission ($\beta L = 8$, $\varepsilon = 1.5$ eV); (II) Simmons with false transition ($\beta L = 16$, $\varepsilon = 3.15$ eV); (III) off-resonant sequential bridge states ($N = 4$, $\varepsilon = 3.63$ eV); and (IV) tail-broadening resonant ($\varepsilon = 1.3$ eV, $\beta L = 10$).

respect to an arbitrary abscissa V^k (where $k = -1$ is the standard TVS form). This leads to

$$\frac{dFN}{d(V^k)} = \left(\frac{G}{J} - \frac{2}{V}\right)\frac{V^{1-k}}{k} = 0 \tag{2}$$

where $G = dI/dV$ is the conductance. Thus eq 2 shows that TVS or a minimum in the Fowler−Nordheim plot occurs at a specific bias, where[20]

$$\left.\left(G - 2\frac{J}{V}\right)\right|_{V=TVS} = 0 \tag{2a}$$

Equation 2 shows that TVS is observed regardless of whether we plot FN (eq 1) against V ($k = 1$), against $1/V$ ($k = -1$), or, for that matter, any other power of V.[6] Note that eq 2a suggests an alternative practical means to extract TVS. If the conductance is measured directly or computed numerically, the function $G - 2J/V$ is easily computed and the bias where it nulls is identical to TVS values extracted from minimizing eq 1. Searching for the null of $G - 2J/V$ has a numerical advantage: it is more robust to noise compared to a process of a minimum search. Moreover, it can also be extrapolated in cases where no min(FN) is observed within the measured bias window, to get an approximation for TVS.

Equation 2 also explains the mathematical meaning of TVS. Equation 2a is actually a form of a differential

equation ($y' = 2y/x$ with a solution $J \propto V^2$. This quadratic solution is applicable only for $V \approx$ TVS, and a "superquadratic" dependence is required for observing a minimum in FN. For example, if the transport relations would behave as $J = aV + bV^2$, the FN function (eq 1) would give a monotonic line (FN = $\ln(b + a/V)$), without any minimum. The TVS point marks the bias where the power law, n, of $J \propto V^n$ changes from $n < 2$ to $n > 2$,[22,23] or the bias where the $J-V$ dependence becomes "superquadratic". This is demonstrated in Figure 2d for the same set of simulated $J-V$ data. The tangential lines have a slope of $n = 2$, and it is clear that the transport curves are tangential to $J \propto V^2$ lines at $V = $ TVS (1.5 V). In other words, TVS is basically a measure of how fast the $J-V$ curve deviates from the "ohmic" approximation[23−25] or how strong the deviation of $G(V)$ from a constant value is, which is commonly used to describe the low-bias transport.[23−25] Naturally, for cases where the bias dependence is stronger than polynomial, e.g., $J \propto e^V$, as in semiconducting electrodes (see below), the deviation from $J \propto V^2$ will occur at very low biases.[26−28]

TVS within the Taylor Expansion. Our analysis so far suggests that TVS is basically an indirect way to measure how nonlinear a given $G-V$ curve is. A much more direct way is to fit $G-V$ curves to generic parabolic relations. Such fitting is an accepted criterion

for identification of tunneling-governed transport through inorganic thin insulators[18,19] and is also clear for the simulated $G-V$ curves of Figure 2c. The three-term Taylor approximation works well for inorganic insulators because it grasps the fundamental physics of back and forth fluxes, which are much larger than the net observed current. The fact that most $G-V$ curves are parabolic within the accessible bias window (see, e.g., ref 5) also explains why the fitting of molecular $J-V$ curves is so deceptive: most tunneling models lead to practically the same generic $G-V$ shape at low to moderate bias range, as shown in Figure 2c.

The coefficients of a generic parabolic fit can be related to the physics of the tunneling process using the Taylor expansion of a detailed tunneling model:

$$G = G(0) + \frac{dG}{dV}\bigg|_0 V + \frac{d^2G}{dV^2}\bigg|_0 \frac{V^2}{2} + \ldots + \frac{d^nG}{dV^n}\bigg|_0 \frac{V^n}{n!} \quad (3)$$

The basic Taylor expansion (eq 3) can be rewritten as the scaled relations[2]

$$G = G_{eq}\left[1 + 2S\frac{V}{V_0} + 3A_2\left(\frac{V}{V_0}\right)^2 + A_3\left(\frac{V}{V_0}\right)^3 \right. $$
$$\left. + A_4\left(\frac{V}{V_0}\right)^4 + \ldots\right] \quad (4)$$

The two scaling parameters are the bias scaling, V_0, and the conductance scaling G_{eq}, which is the equilibrium conductance (i.e., the conductance at $V \to 0$). G_{eq} is widely accepted in analysis of molecular charge transport and commonly expressed as resistance $(1/G_{eq})$.[23−25] G_{eq} is easily determined experimentally, independent of the shape of the $G-V$ curve, which is expressed by the term within the square brackets in eq 4.[1]

Because of the symmetry of back and forth tunneling currents, all odd TyEx coefficients (S, A_3, A_5, …) vanish for symmetric $G-V$ curves. Thus, S measures the asymmetry in the transport and is generally small compared to the coefficient of the third term in the expansion. The A_3 and higher coefficients will be generally ignored here (marked as higher order terms, "O"). Thus the shape of the $G-V$ curve is mostly dominated by the third term, which also serves to experimentally extract V_0. The "2" and "3" prefactors in the scaled conductance expansion (eq 4) are added for convenience, because they disappear in the Taylor expansion of the current density:

$$J \cong G_{eq}V\left(1 + S\frac{V}{V_0} + A_2\left(\frac{V}{V_0}\right)^2 + O\left(\frac{V}{V_0}\right)^n\right) \quad (5)$$

Substituting TyEx expressions for both conductance (eq 4) and current (eq 5) into eq 2a leads to the

following condition for TVS:

$$G - 2\frac{J}{V} \cong G_{eq}\left(-1 + A_2\left(\frac{V}{V_0}\right)^2 + O\left(\frac{V}{V_0}\right)^n\right)\bigg|_{TVS} = 0 \quad (6)$$

Note that eq 6 eliminates the main asymmetry contribution S, and as a result it gives a simple relation between TVS and V_0:

$$TVS = V_0\sqrt{\left[1 - O(TVS/V_0)^n\right]/A_2} \approx V_0 \quad (6a)$$

The prefactor A_2 equals 1 for symmetric junctions and weakly varies with asymmetry (see Table S1). Thus, the identification $TVS \cong V_0$ is valid for nearly symmetric junctions and assumes that the higher order terms can be ignored. Equation 6a implies that TVS is a perturbation of the scaling factor of the applied bias, V_0. Clearly, this is quite a simplification, and higher order terms add corrections to this result.

The validity of the claim that $TVS \approx V_0$ can be experimentally tested by comparing extracted TVS and V_0 values. We used $J-V$ data sets, experimentally measured across monolayers of alkyl-phosphonic acids (APA) made on ultrasmooth oxidized Al (as electrode)[29] and contacted by liquid Hg from the top, as reported elsewhere.[30] The alkyl chains were 8, 10, 12, 14, and 16 carbons long. The bottom Al contact was covered by an inevitable ~3 nm thick Al oxide, but we showed that this nonstoichiometric oxide adds only a minor barrier to transport.[30] The results are shown in Figure 3.

Figure 3a shows the fair linear dependence of G/G_{eq} on V^2; namely, the parabolic approximation eq 4 is reasonable and the asymmetry contribution is negligible. V_0 is extracted from the slope/intercept ratio of a linear fit to such plot, assuming $A_2 = 1$. Figure 3b shows the extracted TVS values as a function of extracted V_0 values. The TVS values are smaller than V_0 by up to 20%, a deviation that increases for shorter chains. We attribute this difference to the higher order terms ("O") neglected in eq 6a. Overall, Figure 3b suggests that the identification of TVS with V_0 is conceptually justified, though not accurate. A qualitative correlation between TVS and the curvature of $G-V$ plots can be inferred also from the work of Guo et al., who compared biphenyl to alkyl dithiol and found that the first has both steeper $G-V$ curves and about half the TVS of the latter.[5]

Finally, Figure 3b shows a clear variation of TVS with molecular length, opposite of what was predicted originally[3] and commonly experimentally observed for Au-contacted alkyl dithiols.[4,32] The high end of TVS values in Figure 3b (~1.2 V) is similar to what was reported by Beebe et al. for alkyl dithiols,[4] but lower than $TVS \approx 1.9$ V reported later for the same molecules.[32] Guo et al. reported that TVS of alkyl dithiols changes from 1.1 to 1.4 V for low- and high-conductance break-junctions (i.e., different distribution
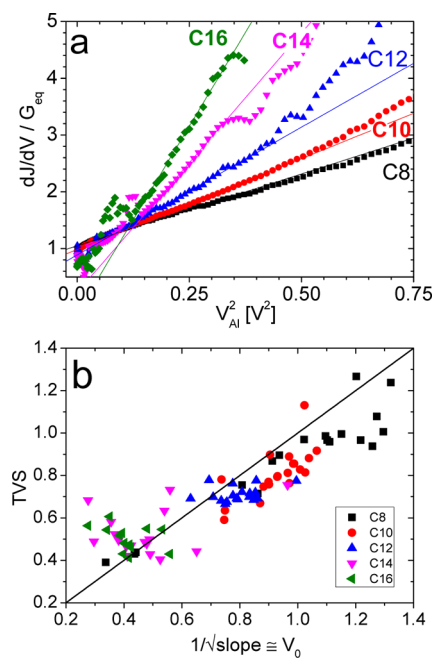
Figure 3. Comparison of Parabolic fit (eq 4) and TVS for transport across monolayers of alkyl-phosphonic acids, showing (a) parabolic fit to selected $G-V^2$ curves; (b) comparison of TVS (Y-axis) and V_0 (X-axis) for all measured junctions. The solid line in (b) represents TVS = V_0. Junctions are comprised of an ultrasmooth Al bottom electrode (30 nm thick on Si),[29] covered with native oxide (3 nm) and a monolayer of alkyl-phosphonic acids. Top contact is made by Hg (~0.3 mm in diameter). See ref 30 for full details. Bias was scanned up to 1 V; thus TVS > 1 was extracted by nulling eq 6, rather than minimizing eq 1. V_0 was extracted from the slope of the linear fit to $G/G_{eq} - V^2$ curves (as in panel a, see eq 4).

bands within thousands of repeated junctions).[5] Length-independent TVS values were considered as a genuine signature of molecular-dominated transport in contrast to, for example, transport across defects.[33] More recent DFT calculations predict TVS to be inversely proportional to length for a trapezoidal potential profile,[10] as we indeed observe in Figure 3b. To track the origin of this length dependence, we have to return to specific tunneling models to give a physical meaning to the generic form of eqs 4 and 6, which we do next.

Taylor Coefficients for Different Tunneling Models. A Taylor's series expansion (TyEx) of WKB-based tunneling was done long ago by Simmons[16] and by Brinkman, Dynes, and Rowell.[17] More recently we followed this approach within the context of *molecular* junctions for both the WKB-based model[1] and off-resonant, sequential tunneling.[2] Here we extend the TyEx method to the Landauer formalism of the general form[11] $J = \frac{2q}{h} \int_{-\infty}^{\infty} T(E)[\mathscr{F}_L - \mathscr{F}_R]dE$, where T is the transmission probability as a function of energy and $\mathscr{F}_{L,R}$ is the Fermi function at the left and right electrodes. Since we are interested in the bias range near 0 V, *i.e.*, far from resonance, the temperature effect can be safely ignored[13] (see also SI), and the zero temperature conductance is

given by (see SI for derivation)

$$G_{(0K)} = \frac{q^2}{h}[(1-\alpha)T(\mu_L) + (1+\alpha)T(\mu_R)] \quad (7)$$

where α is the asymmetry factor, which could vary from -1 to $+1$ and is 0 for the symmetric case,[34] and $\mu_{L,R} = \pm((1 \mp \alpha)/2)qV$ is the position of the Fermi level of the left (grounded) and right (biased) electrodes with respect to the Fermi level at 0 V. Equation 7 is general to any transmission function $T(\mu_{L,R})$ with a step-like potential profile, under the assumption that the temperature effect is negligible, and the density of states is similar at the two electrodes. We comment that considering conductance rather than current does not involve loss of information because the current at 0 V is zero by definition. On the other hand, avoiding one integration step commonly simplifies the mathematical expressions.

Following Huisman *et al.* we use a simple form of the transmission function, that of a single, Lorentzian-shaped level, located ε eV away from the Fermi energy:[11]

$$T(E) = \frac{\exp(-\beta L)}{b + \left(\dfrac{E-\varepsilon}{\varepsilon}\right)^2} \quad (8)$$

where βL is the exponential tunneling decay, replacing here the coupling term. The factor b in eq 8 is $b = (\exp(-\beta L))/(1-\alpha^2)$ and is negligible for $\beta L > \sim 5$ compared to the other denominator term ($\rightarrow 1$, for $E \ll \varepsilon$). The use of $E - \varepsilon$ in the denominator of eq 8 implies that transport *via* the LUMO is assumed, while $E + \varepsilon$ describes HOMO-mediated transport.[20,35] However, in terms of $G-V$ these two options are completely symmetric. The sign convention for α is also arbitrary, and for LUMO-mediated transport, $\alpha > 0$ implies less current under positive bias and *vice versa*.

Substituting eq 8 into eq 7, differentiating with respect to voltage once and twice, and then setting $V = 0$ (see SI for full derivation) provides the coefficients for the TyEx, as listed in Table 1. The table also gives a summary of TyEx coefficients for other relevant tunneling models.

The rightmost column of Table 1 shows that TVS and V_0 are actually not identical. Still, the identification of TVS with V_0 is useful, because it removes the complicated dependence of TVS on uncertain tunneling details. The basic reason for this difference is the fact that TyEx holds near 0 V, while TVS is extracted at quite large bias. The intrinsic energy scale here is the bias scale, V_0. For example, simulations show that parabolic fitting over a bias range limited to $\leq 0.1V_0$ yielded V_0 as expected according to Table 1, but parabolic fitting over a wider bias range leads to increasing deviation. Because TVS $\propto V_0$, by definition TVS will occur outside the region where the three-term TyEx is adequate. In principle, this discrepancy could be

TABLE 1. Parabolic Coefficients for eq 4 for Different Models for Charge Transport across Molecules[a]

model	G_{eq}	V_0	S	V_0/TVS[b]
Simmons/BDR[c]	$G_0(A\beta/8\pi L)e^{-\beta L}$	$9.8\varepsilon/\beta L$	$-\Delta\varepsilon/\varepsilon/4.9$	~1.3
off-resonant, sequential tunneling[d]	$2G_0(\Delta_0/t)^2(\varepsilon/t)^{-2N}$	$2.45\varepsilon/N$	$-\alpha/1.2$	~1.4
tail-broadening resonant tunneling[e]	$[G_0/(1+b)]e^{-\beta L}$	$2\varepsilon(1+b)$	-2α	~1.8

[a] ε (eV) is the barrier height; βL (dimensionless) is the product of length L and tunneling decay coefficient β (for off-resonant tunneling it replaced by N, the number of sites along the bridge); α (dimensionless) is the bias asymmetry; and $G_0 = 2q^2/h$ is the quantum conductance. See SI for higher coefficients. [b] This ratio is similar to 2χ, where $\chi = \varepsilon/TVS$;[10,15] values extracted from the simulation of Figure 2; generally they were similar for a wide range of parameters. [c] A is the area; $\Delta\varepsilon$ is the difference between the left and right barrier heights where ε is the average barrier, according to Brinkman, Dynes, and Rowell (BDR); see ref 17. Similar derivation of TyEx coefficients appears also in refs 1, 2, and 16. [d] Conductance per molecule; N is the number of bridge sites, t is the hopping integral between sites (~1 eV), and Δ_0 is the spectral density of the electrodes (~1 eV), based on eqs 8 and 9 of ref 21. TyEx derivation appears in ref 2 and in the SI. [e] Based on eqs 5 and 6 of ref 11. Full derivation appears in the SI. Note that $b \rightarrow 0$ and can be generally ignored.

made smaller by Taylor expanding around an arbitrary, nonzero bias. However, this leads to rather complicated expressions (cf. Table 1) because only at $V = 0$ do the forward and backward current terms, typical of transport by tunneling, effectively cancel. A better option for keeping the validity of the simple TVS $\approx V_0$ identification is to shift the TVS minima to lower bias values, which is possible by using a modified TVS function (min(ln(J/V^n), $1 < n \leq 2$).[12] This reduces the bias where TVS_n is observed: $TVS_n \approx V_0[(n-1)/(3-n)/A_2]^{1/2}$, ignoring asymmetry and higher order perturbations. Thus using n values approaching 1 will give lower TVS_n values that are closer to TyEx-predicted V_0.[20] This is beneficial also experimentally since often junctions become unstable at high fields,[5] and then the applied bias range is not large enough to include the TVS minimum.

In summary, TVS and V_0 are conceptually the same and show the same trends with respect to junction parameters, though extracted values could differ by ~50%. TVS is probably simpler to extract technically, while V_0 has a clearer mathematical interpretation.

Length Dependence of TVS or V_0. Table 1 compares three tunneling scenarios, and it can be easily extended to any analytical tunneling $J-V$ relations (see, e.g., Table S2 in the SI). Table 1 shows that while both TVS and parabolic fitting are generic, their interpretation is strongly model-dependent. For example, an "insulator" view, where the bias falls on the bridge (Simmons, first row), leads to a V_0 expression that includes a large prefactor (~10) when compared to a "conductor" view, where the bias falls on the contacts (both second and third rows of Table 1) and the prefactor is ~2. In addition, Table 1 shows that for off-resonant tunneling (first and second rows) V_0 should be inversely proportional to the bridge length (βL or N), in contrast to the resonant case (third row), where the tunneling distance has no effect on the shape of the $G-V$ curve,[10] and distance affects only the net conductance (G_{eq}).

In accordance with Table 1, Figure 3 shows a clear dependence of V_0 or TVS on alkyl-chain length, indicated by different color symbols. The clear length effect of Figure 3 and Table 1 is in contrast to an observed length-independent TVS for alkyl dithiols.[4,32] Since both systems are based on an alkyl monolayer, this seems to be a major contradiction. The explanation is that the nature of the contact dictates different tunneling regimes for the two systems.[10] The reason for this lies in the fact that for alkyl-dithiols the transport orbital is located mainly on the S−Au bond[10] due to its large density of states (DOS).[36] This effectively screens the wire[7] and localizes the bias drop to the contacts.[10] On the other hand, for the Al/AlOx-APA/Hg junctions reported here, there is a very small interface DOS because of binding to the oxide on one side and lack of any chemical contact on the Hg side. Thus the observed TVS is inversely proportional to the molecules' length, as predicted for off-resonant tunneling.[10]

One merit of the TyEx view of TVS is the ease at which different tunneling models are compared. Thus Table 1 allows a simple way to choose ε and βL (or N) values for different tunneling models (e.g., the simulated curves of Figure 2) such that they will all give the same TVS value. Similarly, the TyEx expressions for V_0 readily explain how the same Simmons model[8] leads to either a genuine transition or a nontransition minimum in a Fowler−Nordheim presentation (e.g., Figure 2, curves I and II, respectively). Within the Simmons model,[8] a transition into field emission would occur at $V = \varepsilon$; thus, the nature of the observed TVS will depend on which is the smaller value, ε or V_0. The expression for V_0 within the Simmons model (see Table 1) indicates that TVS would mark a real transition into field emission only if $\beta L < 9.8$ (i.e., either very short or highly conjugated molecules). For such low βL values it is also reasonable to assume that less potential drops on the wire, and therefore the low βL condition for length-independent TVS, fits qualitatively with the potential profile argument of Mirjani et al.[10]

Extracting Tunneling Information. Figure 2 clarifies that curve fitting is largely generic and cannot provide much information on specific transport behavior. In this regard TVS or V_0 is merely an effective quantification parameter, like the length-decay coefficient, β,

without a unique physical interpretation. One of the difficulties in translating these effective tunneling parameters (*e.g.*, β, TVS, or V_0) into fundamental physical properties, such as barrier height (ε), coupling to the electrodes (Γ) and along the chain (t), or effective mass (WKB view), is that the experimentally observed parameters depend on different combinations of the physical quantities. An important advantage of the TyEx approach compared to free-fitting is that it forces a separation between the bias scaling, V_0 (or TVS), and the current scaling, G_{eq}. The last can be experimentally determined either from the slope of J *vs* V or by averaging directly measured G values near 0 V. The conductance scaling, G_{eq}, is expected to be dominated by the coupling to the electrodes and the number of transmission channels (or area) in contrast to the bias scaling, V_0, which would be mostly affected by the energy alignment and be insensitive to the coupling.[20,37] The major exception is the length (βL or N), that contributes to both G_{eq} and V_0 in the off-resonant case but only to G_{eq} in the case of resonant-tunneling. Table 1 suggests, therefore, that comparing independently extracted G_{eq} and V_0 values could provide further insight into the specific tunneling model[2,5,37] that cannot be gained from $G-V$ fitting alone.

Table 1 shows that both $\ln(G_{eq})$ and $1/V_0$ depend linearly on N or βL, for off-resonant or Simmons tunneling, respectively.[2] In these cases a plot of $\ln(G_{eq})$ *vs* $1/V_0$ is expected to have a negative slope proportional to the barrier height.[2] In contrast, for resonant tunneling V_0 is predicted to be independent of βL, and thus $\ln(G_{eq})$ *vs* $1/V_0$ should be a vertical line.

Figure 4 shows plots of the conductance and bias scaling parameters of the APA junctions (same as in Figure 3), which show a clear exponential decay, as predicted for off-resonant or Simmons tunneling. Figure 4 suggests that the transport behavior is different for short APAs (C8−C12) and long ones (C14−C16), as was also reported previously.[30] Fitting only the short APAs (dashed line) or the full data (solid line) changed the exponential decay from 8.4 to 4.4. Within the off-resonant, sequential tunneling view (second entry in Table 1) and using $t = 1.68$ eV[10] these slope values translate to $\varepsilon = 3.0$ and 2.4 eV, respectively. Using the Simmons model leads to a lower barrier ($\varepsilon = 0.86$ and 0.45 eV, respectively) because of the much larger prefactor (9.8, *cf*. 2.45) in the V_0 definition (Table 1). Although there is quite a spread, all these values are reasonable, considering the ∼1.6 eV LUMO−Fermi difference, derived from UPS and gap data[38] (setting $t = 0.92$ eV recovers the expected $\varepsilon = 1.6$ eV). Thus Figure 4 indicates a good qualitative agreement between scaling parameters of APA junctions and either Simmons or off-resonant tunneling models, although we stress that the specific values of the extracted barrier height are rather meaningless in our treatment.
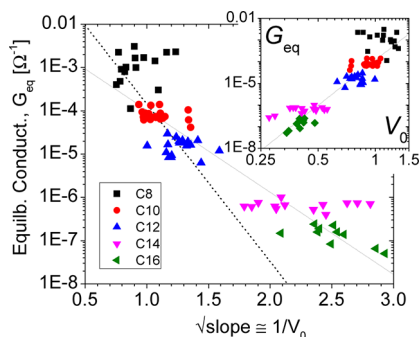

Figure 4. Correlation of G_{eq} and $1/V_0$ values extracted for Al/APA/Hg junctions of varying alkyl chain length. V_0 values were extracted from the slope of linear fits of G/G_{eq} *vs* V^2 (see eq 4 and Figure 3a). G_{eq} values were extracted by averaging the G values in the bias range of 0 to 50 mV. Symbols are experimentally extracted values; lines are exponential fits of G_{eq} *vs* $1/V_0$ over full data range (solid gray line, $G_{eq} = 0.008 \cdot \exp(-4.4/V_0)$) or limited to "short" APAs (C8−C12, dotted line, $G_{eq} = 0.63 \cdot \exp(-8.4/V_0)$). Inset: Log−log plot of G_{eq} *vs* V_0; fitted line shows $G_{eq} \propto V_0^{6.9}$.

For the sake of generality, the inset in Figure 4 shows the same G_{eq} *vs* V_0 data but on a log−log plot, which gives even better correlation than the exponential-decay plot (main panel), with an apparent power law of ∼7. We are not aware of any tunneling model that predicts such relation, but we note that Bâldea suggested that G_{eq} is inversely proportional to TVS[2] (*i.e.*, a power law of −2).[37] Obviously this model does not hold for APA junctions, though it appears to adequately describe tunneling across alkane dithiol[37] and conjugated molecules.[13]

The long APAs (C14, C16) had a rather large spread in their V_0 values, while the G_{eq} distribution was much narrower, with a weak dependence on length (C14, *cf*. C16). Indeed, if V_0 is independent of length, there should be no correlation between V_0 and $\log(G_{eq})$. Qualitatively, this can be explained if the tunneling across long APAs is dominated by the contacts rather than by the bridge (*i.e.*, closer to the resonant-tunneling model; see Table 1). While this conclusion might seem strange because the bridge is actually longer, detailed structural characterizations[30] indicate that the long APAs form much denser monolayers than short ones, and as a result, long APAs are more rigid with a solid-like structure than the short APAs, which are more fluid-like. A distinct change between short and long APAs (same raw data as used for Figures 2 and 3) was also observed in the variation of the exponential length decay coefficient, β, as a function of applied bias.[30,39] Although the HOMO−LUMO gap of isolated alkyl chains is hardly affected by increasing the alkyl length, the β−V analysis suggests that the energy barrier is lower for longer APAs than for shorter APAs. We attributed this observation to considerably more scattering in the constantly fluctuating short APAs compared to a better coherence across the more "frozen" long APAs.[30,40] Thus, the considerable bridge scattering along

short APAs leads to a clear correlation between $\log(G_{eq})$ and V_0, while for the more ordered long APAs this correlation is weaker.

Although the V_0 values for C14 and C16 in Figure 4 appear to be poorly reproducible, their standard deviation (0.15 V) is lower than that reported for TVS values of alkyl dithiol break-junctions (0.25 V).[5] However, the spread in $\ln(G_{eq})$ of alkyl dithiols was even larger than in TVS,[5] while for APAs $\ln(G_{eq})$ showed much better reproducibility than V_0 (see Figure 4). A partial explanation could be that transport across a wide area junction is already area-averaged, while single-molecule experiments reveal the real distribution.[6] It is, however, unclear why this narrowing effect is much more pronounced for the conductance scaling (G_{eq}) than for the bias scaling (V_0). Physically, this implies a larger variance in ε than in the coupling strength. Bâldea has suggested that a large variance in ε could be due to fluctuations in short-range Coulomb interactions at molecule—electrode contacts.[20] This is reasonable for APAs, where the charging state of the phosphonate binding group varies with increasing coordination to the substrate.[30] Furthermore, the ill-controlled amount of hydroxyls on the surface could also affect the exact surface potential.

Nonmetallic Electrodes Lead to Major Artifacts in Voltage Analysis. This last section is concerned with an important consequence of the understanding that TVS is not transition-related but a curvature gauge, namely, the bias effect with nonmetallic electrodes. Nonmetallic contacts are often used in molecular electronics, mostly for large-area junctions. Prominent examples include semiconducting electrodes (e.g., Si[26−28,40−42]), conductive polymers (e.g., PEDOT:PSS[22,43,44]), pyrolyzed photoresist films,[45] and oxidized metals such as Al[30,46] or InGa.[47] The motivation for using these electrodes varies from softness (PEDOT), to lack of chemical interaction (InGa), favorable binding chemistry (Al, carbon), or useful band structure (Si[42]). While such electrodes are commonly sufficiently conducting, to observe a clear molecular effect (e.g., length effect,[44] IETS[26]), they still often dominate the net bias effect on transport. The reason is that transport is dictated by a product of both probability of charge to cross the molecule and probability to find empty/filled states on the leads. Often the bias effect on the population of the leads' DOS is overlooked. While this is justified for metals where the DOS is approximately constant near the Fermi energy, for nonmetallic contacts such an approximation could lead to misinterpretations.

This effect is demonstrated in Figure 5a, showing $J{-}V$ curves for Hg/C16−Si(111) junctions, with n-Si (black line) and p-Si (red line) both heavily doped (doping level 10^{19} cm^{-3}). Data are taken from ref 42, and further experimental details are given there. Despite the nearly degenerately doped Si, the current density of n-Si is 10- to 100-fold smaller than that with p-Si. We explained this by residual band bending in the Si,
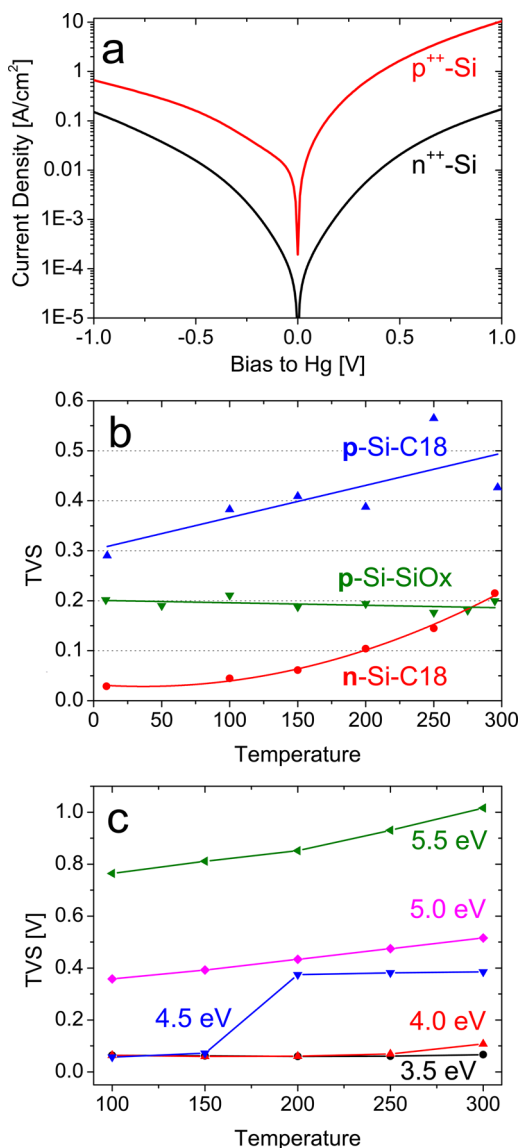

Figure 5. TVS for heavily doped Si electrodes, showing (a) $J{-}V$ curves for Hg/C16−Si(111), doped to $\sim10^{19}$ either n or p (data taken from ref 42); (b) variation of TVS with temperature for different experimentally measured heavily doped Si junctions (see legend, data taken from ref 40); and (c) variation of TVS with metal WF and temperature for simulated $J{-}V$ curves, 10^{19} doped p-Si, 15 Å thick insulator. The transport across the insulator was computed from a two-band transport model, with barriers of 2.4 eV between the molecular LUMO and Si conduction band and 3.6 eV between valence band and HOMO. These values are taken from a UPS/IPES study.[52] The effective mass was set to 0.55 to bring the maximal TVS to 1 V, and the rest of the simulation details and parameters are given in ref 49.

which increases the effective tunneling distance in heavily doped n- compared to p-Si.[42] This additional barrier is not observed in the shape of the $J{-}V$ curve that is more symmetric for lower current (n-Si) than for high current (p-Si). This difference in transport asymmetry is explained by "Esaki-like" diode behavior[48] with LUMO-dominated transport.[42] Thus for nonmetallic electrodes, even if a clear molecular signature is

observed (*e.g.*, length attenuation), there is some bias drop on the nonmetallic lead to maintain the required supply of charge carriers.[41,44]

Therefore, we suggest that the reported very low TVS values (<0.2 V) for Au−S−alkyl−Si (n^{++} or p^{++} doped) junctions[26−28] are due to the bias-varying DOS in the Si. The exact bias partition between the Si and the molecules requires a detailed numerical solution.[41,49] However, for illustrative purposes we consider here the simplest mechanism of current across a thin metal−insulator−semiconductor (MIS) junction by thermionic emission, where the semiconductor is in depletion,[50]

$$J_{MIS} = J_0\, e^{-\beta L} \exp\left(\frac{q}{nkT}V - 1\right) \qquad (9)$$

where *n* is an ideality factor that varies in principle between 1 and 2 and in practice is often larger. Transport using heavily doped Si, as in Figure 5, has a much more complicated form than eq 9. Nevertheless, the *exponential* dependence on bias appears in most semiconductor transport relations. Considering that TVS does not mark a real transition, but rather measures how steep the *J−V* curve is, it is clear that exponential *J(V)* dependence will reach the condition of eq 2 ("superquadratic") already at low biases. Differentiating eq 9 leads to $G_{MIS} = J_{MIS}(q/(nkT))$, and substituting into the minimum definition of eq 2a we get the following prediction for TVS of simplified MIS junctions:

$$TVS_{MIS} \cong 2n\frac{kT}{q} \qquad (9a)$$

Thus TVS for MIS junctions should depend positively on the temperature. This is tested in Figure 5b, showing experimentally extracted TVS values (negative bias on Hg) as a function of temperature for a Hg/C18−Si junction made with both heavily doped n^{++} and p^{++} Si. TVS data for an Hg junction with the same p^{++} Si but with a native oxide rather than alkyl monolayer are also shown (*J−V−T* data taken from ref 40; see therein for experimental details). They show rather low TVS values, in accordance with former findings[26−28] that monotonically increase with temperature, in qualitative agreement with eq 9a. The slope for p^{++} Si−C18 is 6×10^{-4}, which translates into an ideality factor of 3.5, which is reasonable, considering that heavily doped Si is not expected to follow thermionic emission (eq 9). We suggest that observing a temperature effect on TVS is a clear indication that for these junctions the bias effect is not solely dominated by the molecules, and any interpretation of the curve's shape is much more complicated than simple models such as a TVS or TyEx parabola.

Within the accepted "spectroscopy" view of TVS, it was assumed that such low TVS values must originate in some density of surface states,[26] an explanation that we cannot fully rule out for our experimental junctions.[49,51] In order to give further support to the interpretation that low TVS values on the Si electrode originate in a bias drop on the Si, we simulated p^{2+} Si-alkyl/metal junctions, with varying work function of the top metal contact. These simulations[49] are free of surface states. The resulting TVS values (negative bias on metal) are shown in Figure 5c. The simulation clearly shows a strong dependence of TVS on both metal work function (WF) and temperature. Increasing the work function reduces the built-in potential for p-Si (ionization potential was set to 4.9 eV, including a dipole effect of the monolayer), starting from strong inversion (WF = 3.5 eV) and up to full accumulation (WF = 5.5 eV). The simulations show that even for heavily doped Si, only a top metal contact that ensures charge accumulation in the Si enables a full expression of molecular TVS (the "5.5" curve of Figure 5c), and even then, there remains a temperature effect on the TVS.

We conclude that for semiconducting electrodes, even heavily doped ones, TVS includes substrate contributions. This is true for any other *simplistic* quantification of bias effect on molecular transport, where at least one of the electrodes is not metallic. Somewhat similarly, it was reported for a PEDOT:PSS top contact that while transport is length-attenuated by the molecules, the PEDOT:PSS film controls the bias effect.[44] Also for the oxidized Al electrode presented in Figure 3, a slight asymmetry could be observed in the *G−V* plots, which we attribute to possible charging of the thin AlO$_x$ layer. However, the AlO$_x$ was sufficiently conducting not to dominate the bias effect.[30,31] While there are many advantages to the use of nonmetallic substrates, transport is a product of molecular and electrode attenuations, and the last is often bias-dependent.

SUMMARY

In contrast to the original view of TVS as a marker for transition between different transport regimes, we have established the interpretation of TVS as a genuine characteristic of tunneling over the full bias range. In this regard, TVS is a bias-dependent perturbation of V_0, the bias scaling factor. This bias dependence complicates the interpretation of TVS compared to V_0 and does not add much information. Thus, practically TVS $\approx V_0$ and the choice of extracting TVS from a minimum of a logarithmic function or from a polynomial fit is a technical consideration.

Molecular transport models, either resonant or off-resonant, lead to generic parabolic *G−V* relations, which are practically indistinguishable from WKB-derived relations. As a parabola, only three parameters can be experimentally extracted from tunneling *G−V* relations (*cf*. eq 4): (i) the equilibrium conductance, G_{eq}, which scales the conductance; (ii) V_0 or TVS, which scales the applied bias; and (iii) the degree of asymmetry factor, which is measured by S (position of parabola minimum).

This generic parabolic shape of molecular $G-V$ curves is conceptually equivalent to the "diode equation" that provides an effective description of vastly different interfaces and transport regimes. As such, it facilitates data comparison across different experimental test beds and different molecular moieties (conjugated and saturated ones; molecules with or without chemi-contacts/spacers). The strength of the scaled parabolic view over detailed fitting is that it separates experimental observables (G_{eq}, V_0, S) and model-dependent, interpreted parameters (barrier height, coupling, potential profile).

The TyEx-derived coefficients are the bridge between detailed theoretical predictions and the experimental observables. Systematic study of the variation of the parabolic scaling parameters with molecular properties (*e.g.*, length, relative positions of energy levels) and the internal correlation between them (*e.g.*, Figure 4) is the most reliable procedure to gain insight into the specific tunneling model. Finally, realizing that TVS measures where the current becomes "superquadratic" with bias, rather than an energy spectral transition provides a much simpler explanation for nonphysical TVS values observed for semiconducting electrodes and provides a strong cautionary note on applying simplified bias-driven analyses to junctions where the electrodes' DOS could be significantly bias-dependent.

METHODS

Experimental current–voltage data are taken from ref 30 (Figures 3, 4); ref 42 (Figure 5a), and ref 40 (Figure 5b). See therein details for monolayer preparation and transport measurements. MatLab R2010b was used for simulated data of Figure 2 and Figure 5c; the last is based on a model described in ref 49.

Conflict of Interest: The authors declare no competing financial interest.

Supporting Information Available: Includes detailed equations for the three different tunneling models; derivation of Taylor expansion for basic Landauer formalism under zero temperature approximation; additional Taylor coefficients for the asymmetric case and additional two tunneling models. This material is available free of charge *via* the Internet at http://pubs.acs.org.

Note Added after ASAP Publication: This manuscript published ASAP on December 24, 2012. Corrections were made to equation 3 and to Figure 5. The revised version reposted on January 22, 2013.

REFERENCES AND NOTES

1. Vilan, A. Analyzing Molecular Current-Voltage Characteristics with the Simmons Tunneling Model: Scaling and Linearization. *J. Phys. Chem. C* **2007**, *111*, 4431–4444.
2. Vilan, A.; Hikmet, R. A. M. Quantification of Ready-Made Molecular Bilayer Junctions Having Large Structural Uncertainty. *J. Phys. Chem. C* **2008**, *112*, 269–281.
3. Beebe, J. M.; Kim, B.; Gadzuk, J. W.; Frisbie, C. D.; Kushmerick, J. G. Transition from Direct Tunneling to Field Emission in Metal-Molecule-Metal Junctions. *Phys. Rev. Lett.* **2006**, *97*, 026801.
4. Beebe, J. M.; Kim, B.; Frisbie, C. D.; Kushmerick, J. G. Measuring Relative Barrier Heights in Molecular Electronic Junctions with Transition Voltage Spectroscopy. *ACS Nano* **2008**, *2*, 827–832.
5. Guo, S.; Hihath, J.; Díez-Pérez, I.; Tao, N. Measurement and Statistical Analysis of Single-Molecule Current–Voltage Characteristics, Transition Voltage Spectroscopy, and Tunneling Barrier Height. *J. Am. Chem. Soc.* **2011**, *133*, 19189–19197.
6. Bennett, N.; Xu, G.; Esdaile, L. J.; Anderson, H. L.; Macdonald, J. E.; Elliott, M. Transition Voltage Spectroscopy of Porphyrin Molecular Wires. *Small* **2010**, *6*, 2604–2611.
7. Song, H.; Kim, Y.; Jang, Y. H.; Jeong, H.; Reed, M. A.; Lee, T. Observation of Molecular Orbital Gating. *Nature* **2009**, *462*, 1039–1043.
8. Simmons, J. G. Generalized Formula for the Electric Tunnel Effect between Similar Electrodes Separated by a Thin Insulating Film. *J. Appl. Phys.* **1963**, *34*, 1793–1803.
9. Araidai, M.; Tsukada, M. Theoretical Calculations of Electron Transport in Molecular Junctions: Inflection Behavior in Fowler-Nordheim Plot and Its Origin. *Phys. Rev. B* **2010**, *81*, 235114.
10. Mirjani, F.; Thijssen, J. M.; van der Molen, S. J. Advantages and Limitations of Transition Voltage Spectroscopy: A Theoretical Analysis. *Phys. Rev. B* **2011**, *84*, 115402.
11. Huisman, E. H.; Guedon, C. M.; van Wees, B. J.; van der Molen, S. J. Interpretation of Transition Voltage Spectroscopy. *Nano Lett.* **2009**, *9*, 3909–3913.
12. Markussen, T.; Chen, J.; Thygesen, K. S. Improving Transition Voltage Spectroscopy of Molecular Junctions. *Phys. Rev. B* **2011**, *83*, 155407.
13. Bâldea, I. Ambipolar Transition Voltage Spectroscopy: Analytical Results and Experimental Agreement. *Phys. Rev. B* **2012**, *85*, 035442.
14. Bâldea, I. Transition Voltage Spectroscopy: Artefacts of the Simmons Approach. *J. Phys. Chem. Sol.* **2012**, *73*, 1151–1153.
15. Chen, J.; Markussen, T.; Thygesen, K. S. Quantifying Transition Voltage Spectroscopy of Molecular Junctions: Ab Initio Calculations. *Phys. Rev. B* **2010**, *82*, 121412.
16. Simmons, J. G. Low-Voltage Current-Voltage Relationship of Tunnel Junctions. *J. Appl. Phys.* **1963**, *34*, 238–9.
17. Brinkman, W. F.; Dynes, R. C.; Rowell, J. M. Tunneling Conductance of Asymmetrical Barriers. *J. Appl. Phys.* **1970**, *41*, 1915–1921.
18. Rowell, J. M. In *Tunneling Phenomena in Solids*; Burnstein, E.; Lundqvist, S., Eds.; Plenum: New York, 1969; p 273.
19. Duke, C. B. *Tunneling in Solids*; Academic Press: New York, 1969.
20. Bâldea, I. Effects of Stochastic Fluctuations at Molecule–Electrode Contacts in Transition Voltage Spectroscopy. *Chem. Phys.* **2012**, *400*, 65–71.
21. Mujica, V.; Ratner, M. A. Current-Voltage Characteristics of Tunneling Molecular Junctions for Off-Resonance Injection. *Chem. Phys.* **2001**, *264*, 365–370.
22. Wang, G.; Kim, Y.; Na, S.-I.; Kahng, Y. H.; Ku, J.; Park, S.; Jang, Y. H.; Kim, D.-Y.; Lee, T. Investigation of the Transition Voltage Spectra of Molecular Junctions Considering Frontier Molecular Orbitals and the Asymmetric Coupling Effect. *J. Phys. Chem. C* **2011**, *115*, 17979–17985.
23. Kim, B.; Choi, S. H.; Zhu, X. Y.; Frisbie, C. D. Molecular Tunnel Junctions Based on π-Conjugated Oligoacene Thiols and Dithiols between Ag, Au, and Pt Contacts: Effect of Surface Linking Group and Metal Work Function. *J. Am. Chem. Soc.* **2011**, *133*, 19864–19877.

24. Wold, D. J.; Frisbie, C. D. Fabrication and Characterization of Metal-Molecule-Metal Junctions by Conducting Probe Atomic Force Microscopy. *J. Am. Chem. Soc.* **2001**, *123*, 5549–5556.

25. Akkerman, H. B.; Boer, B. d. Electrical Conduction through Single Molecules and Self-Assembled Monolayers. *J. Phys.: Condens. Matter* **2008**, *20*, 013001.

26. Yu, L. H.; Gergel-Hackett, N.; Zangmeister, C. D.; Hacker, C. A.; Richter, C. A.; Kushmerick, J. G. Molecule-Induced Interface States Dominate Charge Transport in Si—Alkyl—Metal Junctions. *J. Phys. D: Appl. Phys.* **2008**, *20*, 374114.

27. Coll, M.; Miller, L. H.; Richter, L. J.; Hines, D. R.; Jurchescu, O. D.; Gergel-Hackett, N.; Richter, C. A.; Hacker, C. A. Formation of Silicon-Based Molecular Electronic Structures Using Flip-Chip Lamination. *J. Am. Chem. Soc.* **2009**, *131*, 12451–12457.

28. Ricoeur, G.; Lenfant, S.; Guerin, D.; Vuillaume, D. Molecule/Electrode Interface Energetics in Molecular Junction: A "Transition Voltage Spectroscopy" Study. *J. Phys. Chem. C* **2012**, *116*, 20722–20730.

29. Levine, I.; Yoffe, A.; Salomon, A.; Li, W.; Feldman, Y.; Cahen, D.; Vilan, A. Epitaxial Two Dimensional Aluminum Films on Silicon (111) by Ultra-Fast Thermal Deposition. *J. Appl. Phys.* **2012**, *111*, 124320.

30. Levine, I.; Weber, S. M.; Feldman, Y.; Bendikov, T.; Cohen, H.; Cahen, D.; Vilan, A. Molecular Length, Monolayer Density, and Charge Transport: Lessons from Al-AlOx/Alkyl-Phosphonate/Hg Junctions. *Langmuir* **2012**, *28*, 404–415.

31. We refer here only to the bias polarity of positive bias on the Al electrode. Such biasing further increases the native potential difference between Hg and Al (work function of 4.5 and 3.8 eV, respectively). Under opposite biasing, the length dependence of TVS is weaker, which might be due to discharging of the AlOx, an issue that is beyond the scope of this paper.

32. Song, H.; Kim, Y.; Jeong, H.; Reed, M. A.; Lee, T. Coherent Tunneling Transport in Molecular Junctions. *J. Phys. Chem. C* **2010**, *114*, 20431–20435.

33. Trouwborst, M. L.; Martin, C. A.; Smit, R. H. M.; Guédon, C. M.; Baart, T. A.; van der Molen, S. J.; van Ruitenbeek, J. M. Transition Voltage Spectroscopy and the Nature of Vacuum Tunneling. *Nano Lett.* **2011**, *11*, 614–617.

34. We prefer this definition of asymmetry over $\eta = 0$ to 1, as in refs 10 and 11, because α nulls for the symmetric case while $\eta = 1/2$ for a symmetric junction. The translation is $\alpha = 2\eta - 1$.

35. Transport by tunneling does not involve actual charging; however, HOMO-mediated transport could be qualitatively viewed as an electron withdrawn from the HOMO ("oxidation"), in contrast to transport *via* the LUMO, which resembles electron injection into the LUMO ("reduction"). In practice it means which of the two levels, HOMO or LUMO, is closer to the Fermi level.

36. Tomfohr, J. K.; Sankey, O. F. Complex Band Structure, Decay Lengths, and Fermi Level Alignment in Simple Molecular Systems. *Phys. Rev. B* **2002**, *65*, 245105.

37. Bâldea, I. Interpretation of Stochastic Events in Single-Molecule Measurements of Conductance and Transition Voltage Spectroscopy. *J. Am. Chem. Soc.* **2012**, *134*, 7958–7962.

38. Unpublished UPS spectra (by A. Kahn, Princeton) show a Fermi—HOMO difference of 5.9 eV; assuming a HOMO—LUMO gap of 7.5 eV, leads to a LUMO—Fermi difference of 1.6 eV.

39. The $\beta^2(V)$ dependence in ref 30 was parabolic and not linear (Simmons), which could be explained by two-band transport rather than single-level-dominated transport. Nevertheless, this issue does not affect much the derivations of Table 1, except that the extracted barrier height, ε, is lower than the real level separation, ε_0: $\varepsilon = \varepsilon_0(1 - \varepsilon_0/E_g)$.

40. Shpaisman, H.; Seitz, O.; Yaffe, O.; Roodenko, K.; Scheres, L.; Zuilhof, H.; Chabal, Y. J.; Sueyoshi, T.; Kera, S.; Ueno, N.; *et al.* Structure Matters: Correlating Temperature Dependent Electrical Transport through Alkyl Monolayers with Vibrational and Photoelectron Spectroscopies. *Chem. Sci.* **2012**, *3*, 851–862.

41. Vilan, A.; Yaffe, O.; Biller, A.; Salomon, A.; Kahn, A.; Cahen, D. Molecules on Si: Electronics with Chemistry. *Adv. Mater.* **2010**, *22*, 140–159.

42. Yaffe, O.; Qi, Y.; Scheres, L.; Puniredd, S. R.; Segev, L.; Ely, T.; Haick, H.; Zuilhof, H.; Vilan, A.; Kronik, L.; *et al.* Charge Transport across Metal/Molecular (Alkyl) Monolayer-Si Junctions Is Dominated by the LUMO Level. *Phys. Rev. B* **2012**, *85*, 045433.

43. Akkerman, H. B.; Naber, R. C. G.; Jongbloed, B.; Hal, P. A. v.; Blom, P. W. M.; Leeuw, D. M. d.; Boer, B. d. Electron Tunneling through Alkanedithiol Self-Assembled Monolayers in Large-Area Molecular Junctions. *Proc. Natl. Acad. Sci.* **2007**, *104*, 11161–11166.

44. Kronemeijer, A. J.; Katsouras, I.; Huisman, E. H.; van Hal, P. A.; Geuns, T. C. T.; Blom, P. W. M.; de Leeuw, D. M. Universal Scaling of the Charge Transport in Large-Area Molecular Junctions. *Small* **2011**, *7*, 1593–1598.

45. Sayed, S. Y.; Fereiro, J. A.; Yan, H.; McCreery, R. L.; Bergren, A. J. Charge Transport in Molecular Electronic Junctions: Compression of the Molecular Tunnel Barrier in the Strong Coupling Regime. *Proc. Natl. Acad. Sci.* **2012**, *109*, 11498–11503.

46. Novak, M.; Jäger, C. M.; Rumpel, A.; Kropp, H.; Peukert, W.; Clark, T.; Halik, M. The Morphology of Integrated Self-Assembled Monolayers and Their Impact on Devices - A Computational and Experimental Approach. *Org. Electron.* **2010**, *11*, 1476.

47. Chiechi, R. C.; Weiss, E. A.; Dickey, M. D.; Whitesides, G. M. Eutectic Gallium—Indium (EGaIn): A Moldable Liquid Metal for Electrical Characterization of Self-Assembled Monolayers. *Angew. Chem., Int. Ed.* **2008**, *47*, 142–144.

48. Esaki, L.; Stiles, P. J. New Type of Negative Resistance in Barrier Tunneling. *Phys. Rev. Lett.* **1966**, *16*, 1108–1111.

49. Toledano, T.; Biller, A.; Bendikov, T.; Cohen, H.; Vilan, A.; Cahen, D. Controlling Space Charge of Oxide-Free Si by in Situ Modification of Dipolar Alkyl Monolayers. *J. Phys. Chem. C* **2012**, *116*, 11434–11443.

50. Card, H. C.; Rhoderick, E. H. Studies of Tunnel MOS Diodes 1. Interface Effects in Silicon Schottky Diodes. *J. Phys. D: Appl. Phys.* **1971**, *4*, 1589–1601.

51. Segev, L.; Salomon, A.; Natan, A.; Cahen, D.; Kronik, L.; Amy, F.; Chan, C. K.; Kahn, A. Electronic Structure of Si(111)-Bound Alkyl Monolayers: Theory and Experiment. *Phys. Rev. B* **2006**, *74*, 165323.

52. Salomon, A.; Boecking, T.; Seitz, O.; Markus, T.; Amy, F.; Chan, C.; Zhao, W.; Cahen, D.; Kahn, A. What Is the Barrier for Tunneling through Alkyl Monolayers? Results from n- and p-Si-Alkyl/Hg Junctions. *Adv. Mater.* **2007**, *19*, 445–450.

ARTICLE